Plasmonic structure integrated single-photon detectors for absorptance and polarization contrast maximization

M. Csete*, A. Szenes*, D. Maráczi*, B. Bánhelyi**, T. Csendes** and G. Szabó*

* Department of Optics and Quantum Electronics, University of Szeged, H-6720 Szeged, Dóm tér 9, Hungary, mcsete@physx.u-szeged.hu
**Department of Computational Optimization, University of Szeged, H-6720 Szeged, Árpád tér 2, Hungary, banhelyi@inf.u-szeged.hu

ABSTRACT

Numerical optimization was performed via COMSOL to maximize p-polarized absorptance and p-to-s polarized absorptance ratio - nominated as polarization contrast - of superconducting nanowire single photon detectors (SNSPDs). Four different types of SNSPDs were integrated with various plasmonic structures capable of influencing the polarized light absorptance inside the superconducting nanowires. Half- and one-wavelength-scaled periodic structures were appropriate to initiate unique nanophotonical phenomena. Here we present that 95.1% absorptance and 1.8 □10^{13} polarization contrast can be achieved and show conditional polarization contrasts reachable by meeting criteria regarding the minimal p-polarized absorptance.

Keywords: SNSPD, plasmonic phenomena, absorptance enhancement, polarization contrast, dispersion diagrams

1 INTRODUCTION

Superconducting nanowire single-photon detectors (SNSPDs) are important for single-photon detection at 1550 nm infrared wavelength in quantum information processing (QIP), telecommunication and astronomy [1, 2]. Absorptance of single-photons with a specific polarization has to be maximized to read-out encoded information with good fidelity in QIP. According to our previous studies the configuration of linear plasmonic structure integrated SNSPDs, which make possible to maximize p-polarized absorptance, is a device structure dependent tilting in S-orientation (at 90° azimuthal angle) [3-5].

A-SNSPD configurations capable of maximizing p-polarized light absorptance, and P-SNSPDs with potential to maximize p-to-s absorptance ratio, referred as polarization contrast, were determined for four different plasmonic structure integrated detectors. The studied device types are nano-cavity-array (NCAI-), nano-cavity-deflector-array (NCDAI-), nano-cavity-double-deflector-array (NCDDAI-) and nano-cavity-trench-array (NCTAI-) integrated SNSPDs (Fig. 1a-d). The inspected devices consisted of integrated periodic patterns with half- and one-wavelength periodicity, which result in Bragg scattering and Rayleigh phenomenon, respectively. In our present study the polar angle was varied with the geometrical parameters in S-orientation of the integrated SNSPDs to determine the optimal configuration (Fig. 1e). An in-house developed GLOBAL optimization methodology was implemented using LiveLink for MATLAB in RF module of COMSOL to determine the optimal A- and P-SNSPD configurations. In case of C-SNSPDs optimization has been performed for polarization contrast by setting a condition regarding the p-polarized absorptance that have to be parallel met. The criterion regarding the minimal p-polarized absorptance was varied with 0.25% steps in 3.0% interval of the maximal absorptance reached in A-SNSPDs.

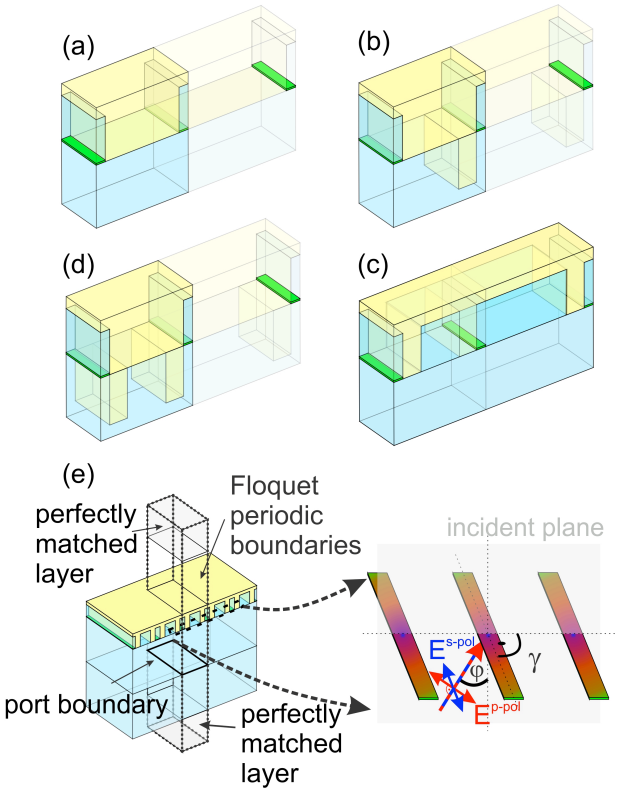

Figure 1: Schematics of (a) NCAI-, (b) NCDAI-, (c) NCDDAI- and (d) NCTAI-SNSPD device geometries, (e) computational and illumination methodology to obtain the optical response.

2 RESULTS

In half-wavelength-scaled NCAI-A-SNSPD the highest 94.2% absorptance is reached at the 76.4° plasmonic Brewster angle (PBA), while a moderate $2.4\square10^2$ polarization contrast is achieved at 85.0° tilting (Fig. 2a). In NCAI-P-SNSPD $6.4\square10^2$ polarization contrast can be achieved at 85.0° tilting, which is accompanied by 65.6% p-polarized absorptance. The 83.0° orientation, where the absorptance reaches the 67.7% maximal value, is close to the 84.9° PBA of the wavelength-scaled device (Fig. 2a).

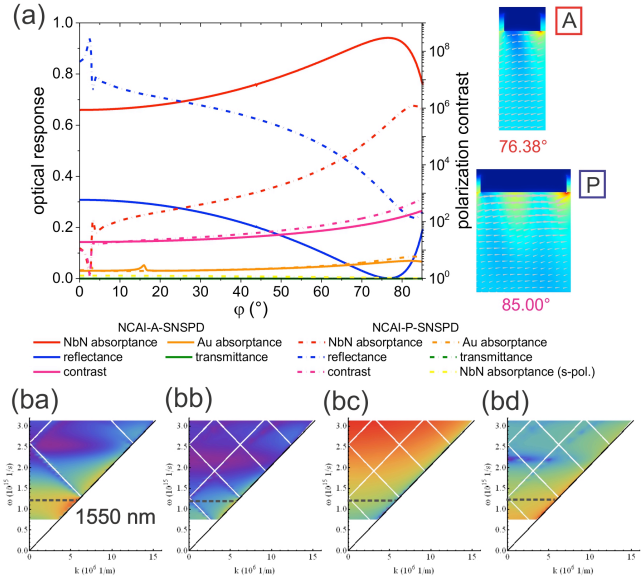

Figure 2: (a) Polar angle dependent optical response of NCAI-A- and NCAI-P-SNSPD. Dispersion diagrams of (ba) p-polarized light absorptance of NCAI-A-SNSPD; (bb) p-polarized light absorptance, (bc) s-polarized light absorptance and (bd) polarization contrast of NCAI-P-SNSPD. Insets: near field of (A) NCAI-A-SNSPD and (P) NCAI-P-SNSPD at absorptance and contrast maxima respectively.

The light is tunneled at tilting corresponding / close to PBA in NCAI-A-SNSPD / NCAI-P-SNSPD, and quarter-wavelength nano-cavities ensure **E**-field confinement in both optimized devices. The near-field is more strongly enhanced at the leading-sides of the nano-cavities, however the **E**-field distribution shows an additional antinode below the gold segment in the NCAI-P-SNSPD (insets A and P in Fig. 2a). This **E**-field distribution is responsible for the larger competitive absorptance in gold.

The comparison of the dispersion characteristics of NCAI-A-SNSPD and NCAI-P-SNSPDs shows that the PBA appears close to the first and second Brillouin zone boundary (Fig. 2ba and bb). The large polarization contrast is promoted by the small s-polarized absorptance close to the second BZ boundary in NCAI-P-SNSPD (Fig. 2bc and bd). The global minimum and local maximum on the NbN absorptance originates from the coupling of the plasmonic and photonic modes in -1 order on the integrated pattern.

In the half-wavelength-scaled NCDAI-A-SNSPD the highest 94.7% absorptance is reached at 0.04°, while the highest $1.5\square10^3$ polarization contrast is achieved again at 85.0° tilting (Fig. 3a). Significantly larger $6.9\square10^{11}$ contrast is reached at the same 85.0° tilting in the wavelength-scaled NCDAI-P-SNSPD, which is accompanied by 64.5% p-polarized absorptance (Fig. 3a). The 81.6° tilting, where NCDAI-P-SNSPD exhibits the highest 68.9% p-polarized absorptance, is close to the 84.8° PBA of the integrated device.

Local field enhancement is observable at the deflectors corners in NCDAI-A-SNSPD, in which quarter-wavelength cavity ensures **E**-field enhancement around the NbN segments (inset A in Fig. 3a). However, the leaving side of the deflector is significantly more shiny in NCDAI-P-SNSPD, moreover the width of the deflector equals to the width of the gold segment in NCDAI-P-SNSPD, proving that the enhanced polarization contrast is due to the robust, in-substrate-deepened gold segments presence (inset P in Fig. 3a). The number of **E**-field antinodes is two both vertically and horizontally, the former is in accordance with that the extended cavity is half-wavelength-scaled, while the latter indicates that surface modes are coupled on the integrated pattern.

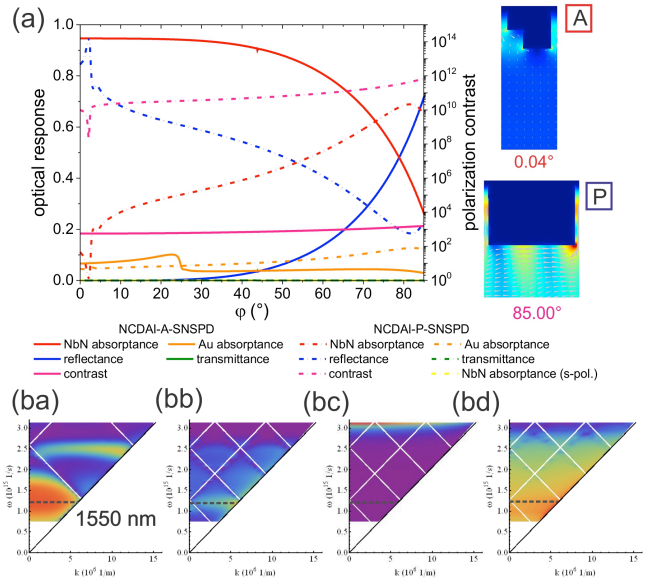

Figure 3: (a) Polar angle dependent optical response of NCDAI-A- and NCDAI-P-SNSPD. Dispersion diagrams of (ba) p-polarized light absorptance of NCDAI-A-SNSPD; (bb) p-polarized light absorptance, (bc) s-polarized light absorptance and (bd) polarization contrast of NCDAI-P-SNSPD. Insets: near-field of (A) NCDAI-A-SNSPD and (P) NCDAI-P-SNSPD at absorptance and contrast maxima respectively.

The comparison of the dispersion characteristics shows, that the NCDAI-A exhibits large p-polarized absorptance inside a wide plasmonic pass band, while the NCDAI-P-SNSPD exhibits significant p-polarized absorptance inside a narrow region close to the second BZ boundary (Fig. 3ba and bb). The large contrast can be achieved due to the depressed s-polarized absorptance in NCDAI-P-SNSPD (Fig. 3bc and bd). The global minimum and local maximum on the NbN absorptance originates from the coupling of the plasmonic and photonic modes in -1 order on the integrated pattern. These results indicate that different nanophotonical phenomena play important role in optimal NCDAI-A-SNSPD and NCDAI-P-SNSPDs in absorptance/polarization contrast maximization.

In the half-wavelength-scaled NCDDAI-A-SNSPD the highest 94.6% absorptance is reached at 60.9°, while the highest $2.7\square10^3$ polarization contrast is achieved again at 85.0° tilting (Fig. 4a). Significantly larger $1.8\square10^{13}$ contrast is reached at the same 85° tilting in the wavelength-scaled NCDDAI-P-SNSPD, however this is accompanied by reduced 70.4% p-polarized absorptance (Fig. 4a). The contrast maximum appears closer to the 85.2° PBA of the integrated device, however NCDDAI-P-SNSPD exhibits the highest 70.6% p-polarized absorptance at 84.4° tilting.

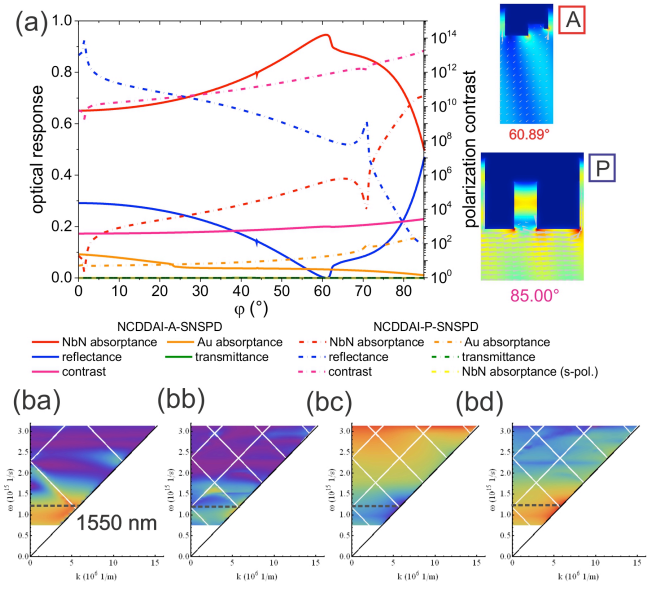

Figure 4: (a) Polar angle dependent optical response of NCDDAI-A- and NCDDAI-P-SNSPD. Dispersion diagrams of (ba) p-polarized light absorptance of NCDDAI-A-SNSPD; (bb) p-polarized light absorptance, (bc) s-polarized light absorptance and (bd) polarization contrast of NCDDAI-P-SNSPD. Insets: near-field of (A) NCDDAI-A-SNSPD and (P) NCDDAI-P-SNSPD at absorptance and contrast maxima respectively.

Stronger local field enhancement is observable at the leaving side of the deflectors in NCDDAI-A-SNSPD, in which quarter-wavelength cavities ensure **E**-field enhancement around the NbN segments (inset A in Fig. 4a). The leaving side of the first deflector and both corners of the second deflector are more shiny in NCDDAI-P-SNSPD (inset P in Fig. 4a). The length of the deflectors almost equal in NCDDAI-P-SNSPD, and there is only a small distance in between them. This is in accordance with that polarization contrast enhancement is promoted again by robust, in-substrate-deepened gold segments. The number of **E**-field antinodes is two vertically and three horizontally, the former indicates that the extended cavity is three-quarter-wavelength-scaled, while the latter shows that larger number of surface modes is coupled on the integrated pattern.

The comparison of the dispersion characteristics shows, that the NCDDAI-A-SNSPD exhibits large p-polarized absorptance inside a crossing bands of cavity and propagating plasmonic modes, while the NCDDAI-P-SNSPD possesses significant p-polarized absorptance inside a narrow region close to the second BZ boundary (Fig. 4ba and bb). The large polarization contrast is achieved due to the depressed s-polarized absorptance in NCDDAI-P-SNSPD (Fig. 4bc and bd). The global and local minimum on the NbN absorptance originates from the coupling of the photonic and plasmonic modes in 1 and -2 order on the integrated pattern. These results again indicate that different nanophotonical phenomena play important role in the optimal NCDDAI-A-SNSPD and NCDDAI-P-SNSPDS in absorptance and polarization contrast maximization.

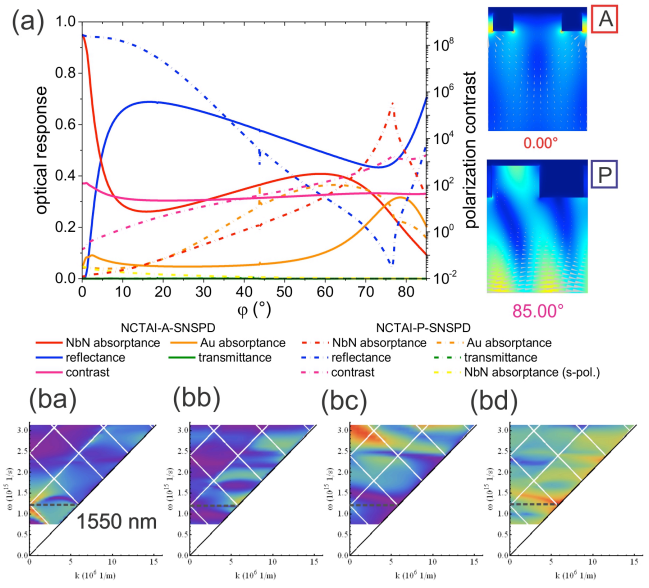

Figure 5: (a) Polar angle dependent optical response of NCTAI-A- and NCTAI-P-SNSPD. Dispersion diagrams of (ba) p-polarized light absorptance of NCTAI-A-SNSPD; (bb) p-polarized light absorptance, (bc) s-polarized light absorptance and (bd) polarization contrast of NCTAI-P-SNSPD. Insets: near-field of (A) NCTAI-A-SNSPD and (P) NCTAI-P-SNSPD at absorptance and contrast maxima respectively.

In case of NCTAI-SNSPD both A and P type optimal configurations correspond to a wavelength-scaled integrated pattern.

Important advantage is that the highest 95.1% absorptance is reached in NCTAI-A-SNSPD at 0°, moreover the highest $1.2\square10^2$ polarization contrast is achieved at 1° tilting, namely close to perpendicular incidence (Fig. 5a). Enhanced $1.9\square10^3$ contrast is reached at 85.0° tilting in the wavelength-scaled NCTAI-P-SNSPD, which is accompanied by strongly reduced 31.4% p-polarized absorptance (Fig. 5a). The polarization contrast maximum appears close to the 85.2° PBA of the integrated device, however NCTAI-P-SNSPD exhibits the highest 69.1% p-polarized absorptance at 76.6° tilting.

Stronger local field enhancement is observable at the NbN-filled cavity-side of the gold segments in NCTAI-A-SNSPD, in which quarter-wavelength cavity ensures **E**-field enhancement around the superconducting segments (inset A in Fig. 5a). There is a local field enhancement inside the trench, which causes competitive gold absorptance (inset P in Fig. 5a). The cavities are half-wavelength-scaled, which causes that the **E**-field is not efficiently confined around the NbN segments in NCTAI-P-SNSPD.

The comparison of the dispersion characteristics shows, that the NCTAI-A-SNSPD exhibits large p-polarized absorptance inside an inverted minigap, while the NCTAI-P-SNSPD exhibits significant p-polarized absorptance inside a narrow region close to the second BZ boundary (Fig. 5ba and bb). The **E**-field is maximized in NCTAI-A-SNSPD due to the Rayleigh phenomenon on the integrated pattern and the large NbN absorptance is promoted by minimized competitive gold absorptance (Fig. 5bc and bd). The large polarization contrast is again promoted by the depressed s-polarized absorptance in NCTAI-P-SNSPD. The global maximum on the NbN absorptance originates from the coupling of the photonic modes in -2 order on the integrated pattern. These results prove that different nanophotonical phenomena make possible absorptance/polarization contrast maximization in optimal NCTAI-A-SNSPD and NCTAI-P-SNSPDS.

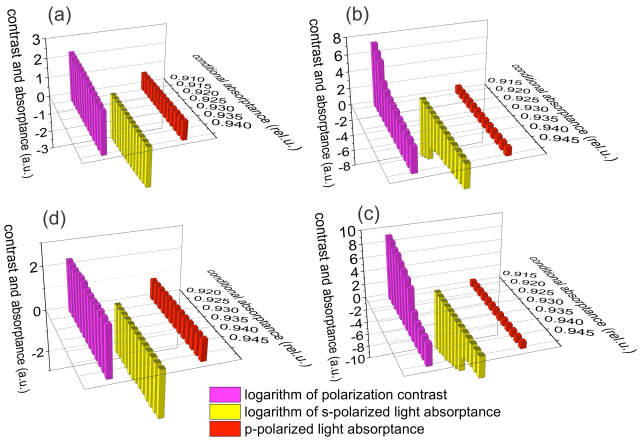

Figure 6: Polarization contrast, s-polarized light and p-polarized light absorptance of (a) NCAI-, (b) NCDAI-, (c) NCDDAI- and (d) NCTAI-C-SNSPD as a function of conditional absorptance.

In C-SNSPD devices $3.2\square10^2$ / $3.0\square10^7$ / $2.2\square10^9$ / $2.6\square10^2$ polarization contrasts are reachable at the expense of 3.0% absorptance decrease. The polarization contrast exhibits correlation with the (extended) cavity length/width, (extended) cavity length in quarter wavelength units and NbN/Au volume fraction ratio (Fig. 6).

ACKNOWLEDGEMENT

The research was supported by National Research, Development and Innovation Office-NKFIH through project "Optimized nanoplasmonics" K116362. Mária Csete acknowledges that the project was supported by the János Bolyai Research Scholarship of the Hungarian Academy of Sciences.

REFERENCES

[1] R. H. Hadfield: "*Single-photon detectors for optical quantum information applications*", Nature Photonics **3** (2009) 696.

[2] F. Najafi, J. Mower, N. C. Harris, F. Bellei, A. Dane, C. Lee, X. Hu, P. Kharel, F. Marsili, S. Assefa, K. K. Berggren, D. Englund, "*On-chip detection of non-classical light by scalable integration of integration of single-photon detectors*", Nature Communications, Vol. **6**, 5873, 2014

[3] M. Csete, A. Szalai, Á. Sipos, G. Szabó, "*Impact of polar-azimuthal illumination angles on efficiency of nano-cavity-array integrated single-photon detectors*", Optics Express, Vol. **20/15**, 17065, 2012.

[4] M. Csete, Á. Sipos, A. Szalai, G. Szekeres, F. Najafi, G. Szabó, K. K. Berggren: „*Improvement of infrared single-photon detectors absorptance by integrated plasmonic structures*", Nature Scientific Reports **3** (2013) 2406.

[5] M. Csete, G. Szekeres, A. Szenes, A. Szalai and G. Szabó: "*Plasmonic Structure Integrated Single-Photon Detector Configurations to Improve Absorptance and Polarization Contrast*", Sensors, **15(2)**, 3513-3539 (2015).